

Doppler Shift of Self-Reflected Optical Pulses at an Interface: Dynamic Nonlinear Optical Skin Effect

W. Forsyiaik,* R. G. Flesch, and J. V. Moloney

Arizona Center for Mathematical Sciences, Department of Mathematics, University of Arizona, Tucson, Arizona 85721

E. M. Wright

Optical Sciences Center, University of Arizona, Tucson, Arizona 85721

(Received 10 October 1995)

We introduce the dynamic nonlinear optical skin effect in which a pulse incident on a saturable absorbing interface is self-reflected from a moving absorption front. The motion of the front causes the self-reflected wave to be redshifted by the Doppler effect, which in turn serves as an experimentally observable signature for the front propagation. [S0031-9007(96)00202-5]

PACS numbers: 42.65.-k, 41.20.Jb, 42.50.Gy

In the linear optical skin effect a pulse incident from air is reflected from a highly absorbing interface after penetrating only a fraction of a wavelength into the absorbing medium, this distance being the skin depth [1,2]. The skin effect is therefore of fundamental importance in understanding the electrodynamics of pulse propagation at condensed matter interfaces, such as metals for field frequencies below the plasma frequency [2], and semiconductors with highly absorbing excitonic features [3]. In addition, it belongs to an important class of optical problems for which the notion of an electromagnetic field envelope varying slowly on the scale of a wavelength simply does not apply. The skin effect cannot be understood on the basis of envelope equations but is rather a consequence of Maxwell's equations for the interface.

In this Letter we introduce the dynamic nonlinear optical skin effect for pulses and elucidate the underlying physics. In the nonlinear skin effect a high intensity pulse is incident upon a nonlinear absorbing interface. Broadly speaking, saturation of the absorption allows the incident field to penetrate beyond the linear skin depth into the medium, and this causes an absorption front to propagate into the medium which separates the regions of low (saturated) and high (unsaturated) absorption. The front is excited by the incident pulse which is in turn reflected from the sharp absorption front, yielding a self-reflected pulse [4]. Thus the absorption front acts as a moving mirror from which the pulse is self-reflected, and the pulse suffers a redshift due to the Doppler effect [5].

Continuous wave (cw) self-reflection from stationary absorption fronts for plane wave [4] and transverse Gaussian [7] fields incident at sharp and smooth [6] interfaces has been studied theoretically but not experimentally verified so far. In part, this is due to the extremely high absorption and strong saturation required for its manifestation, but the difficulty of obtaining good experimental signatures should not be overlooked. Here we explore the transient regime using the two-level Maxwell-Bloch equations. In particular, we show that moving fronts are excited by the incident pulse [8,9] and that the self-reflected pulse bears clear

spectral signatures due to the Doppler effect, which should be observable experimentally.

We consider the time-dependent propagation of a linearly polarized plane electromagnetic wave incident on a nonlinear medium composed of two-level systems. For propagation along the z axis, and taking the electric field polarized along the x axis, Maxwell's curl equations take the form [1,2]

$$\frac{\partial B_y}{\partial t} = -\frac{\partial E_x}{\partial z}, \quad \frac{\partial D_x}{\partial t} = -\frac{\partial H_y}{\partial z}, \quad (1)$$

where $B_y = \mu_0 H_y$. The specification of the problem is completed with the constitutive relation $D_x = \epsilon_0 E_x + P_x$, where P_x is the optical polarization. To elucidate the basic physics we employ a two-level model to describe the optical response with lower electronic state $|1\rangle$ and upper state $|2\rangle$. The Bloch equations are then (see, for example, Ref. [10])

$$\begin{aligned} \frac{\partial \rho_{21}}{\partial t} + (\gamma_2 + i\omega_{21})\rho_{21} &= i\frac{pE}{\hbar}n, \\ \frac{\partial n}{\partial t} + \gamma_1(n-1) &= 2i\frac{pE}{\hbar}(\rho_{21} - \rho_{21}^*), \end{aligned} \quad (2)$$

where ρ_{21} is the off-diagonal density matrix element, $n = \rho_{11} - \rho_{22}$ is the population difference between the lower and upper states, ω_{21} is the transition frequency, p is the dipole moment in the field direction, and γ_1 and γ_2 are phenomenological damping constants for the population and polarization, respectively. The polarization due to the atoms is then given by $P_x = N(z)p(\rho_{21} + \text{c.c.})$, with $N(z)$ the density of two-level systems which varies along z in general.

Equations (1) and (2) are solved using a standard discretization scheme described by Yee [11] and the Bloch equations integrated in time using a fourth-order Runge-Kutta method. The system of equations was solved with the initial condition on the field

$$E_x(z, t=0) = E_0 \cos[2\pi\omega(z-z_0)/c]e^{-(z-z_0)^2/(ct_0)^2}, \quad (3)$$

along with a similar expression for B_y with $B_0 = E_0/c$. Here E_0 is the peak input electric field, $\omega = 2\pi c/\lambda_0$ is the central pulse frequency, $\tau_0 = 2t_0$ is the full width at the $1/e^2$ points of the pulse intensity profile in time units, and z_0 is the position of the pulse center at $t = 0$. The nonlinear interface was imposed by tailoring the density profile $N(z) = \theta(z - z_{\text{int}})N_0$, with z_{int} the longitudinal position of the interface. The medium was initialized using $\rho_{21} = 0$, and $n = 1$ in the medium. When initializing the field, we ensured that the field protruded negligibly into the nonlinear medium at $t = 0$.

In the limit of cw fields, as previously studied by Roso-Franco [4], the self-reflected wave arises when the normalized parameters,

$$\psi = \frac{p^2 N}{\epsilon_0 \hbar \gamma_2}, \quad F = \frac{p E_0}{\hbar (\gamma_1 \gamma_2)^{1/2}}, \quad (4)$$

are both greater than unity. Physically, ψ determines the linear absorption per wavelength, $\alpha \lambda_0 = 2\pi\psi$, and this quantity should be greater than unity for the linear skin effect. For saturation of the absorption and self-reflection, $F > 1$ is required since F^2 is the peak incident field intensity normalized to the cw saturation intensity.

We consider the transient regime in which the incident pulse width t_0 is much shorter than the population relaxation time $T_1 = \gamma_1^{-1}$, but longer than the polarization dephasing time $T_2 = \gamma_2^{-1}$, $T_1 \gg t_0 > T_2$. For concreteness we adopt the following specific parameters, $\omega = \omega_{12} = 2 \times 10^{15} \text{ rad s}^{-1}$, $t_0 = 300 \text{ fs}$, $T_1 = 0.5 \text{ ns}$, $T_2 = 50 \text{ fs}$, $p = 5ea_0 = 4 \times 10^{-29} \text{ C m}$, $N_0 = 4 \times 10^{19} \text{ cm}^{-3}$, and $z_0 = -225 \mu\text{m}$. For these parameters, $\psi = 3.8$ so that the linear skin effect is expected at low input intensities. We have numerically verified that this is indeed the case, and the input pulse suffers minimal distortion in profile or spectrum upon reflection.

Figures 1(a) and 1(b) show an example of the calculated pulses at two different times for a peak input field of $E_0 = 1.6 \times 10^8 \text{ V/m}$. Although our calculations employ the full field, we display only the envelope obtained from joining the peaks as shown by the solid line, since it is not possible to resolve the carrier in the plots. The field strength is associated with the scale shown on the left-hand side of the plots. In Fig. 1(a) for $t = 1.68 \text{ ps}$ the peak of the input pulse has not yet reached the interface at $z_{\text{int}} = 400 \mu\text{m}$, but one can clearly see the leading edge of the pulse is penetrating only a short distance into the interface, as expected for the skin effect. The dashed line in Fig. 1(a), which is associated with the right-hand scale, is the local wavelength for the field. This is determined numerically by calculating the local wave number K via $K^2 \approx -E_x''/E_x$, where a prime signifies a z derivative, and converting to wavelength. In Fig. 1(a) the local wavelength remains constant at the input value $\lambda_0 = 942 \text{ nm}$. In contrast, Fig. 1(b) shows the field profile at a later time $t = 2.75 \text{ ps}$ following reflection from the interface [for times between the results shown in Figs. 1(a) and 1(b), the field profile shows strong ringing due to interference

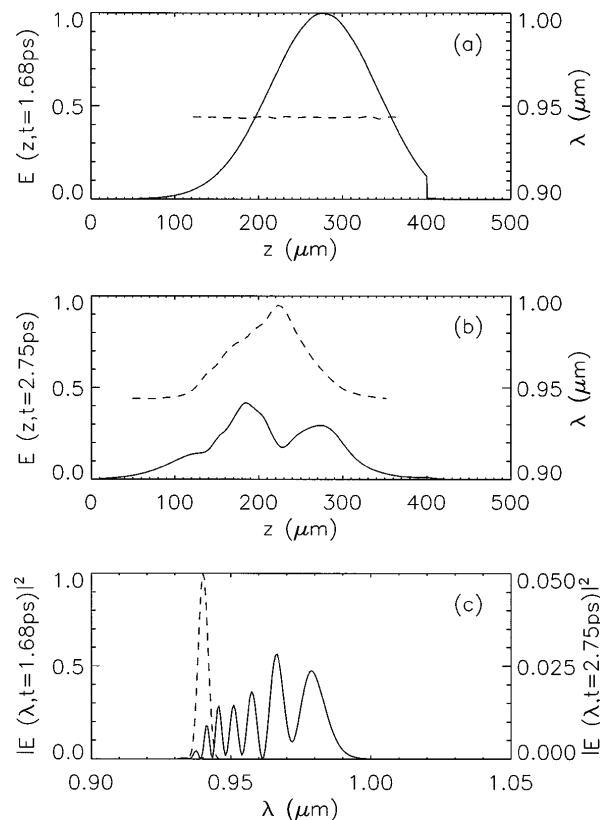


FIG. 1. Calculated field profiles (solid lines) for $E_0 = 1.6 \times 10^8 \text{ V/m}$ and (a) $t = 1.68 \text{ ps}$ before the field enters the interface at $z_0 = 400 \mu\text{m}$, and (b) $t = 2.75 \text{ ps}$ following reflection from the interface. In plots (a) and (b) we show only the envelope obtained from joining the field peaks. The field strength is associated with the left-hand scale and is normalized to unity. The dashed lines in (a) and (b) show the corresponding local wavelength over the pulse, and are associated with the right-hand scale. (c) The corresponding pulse spectra. The input spectrum is shown dashed and is associated with the left-hand scale.

between the incident and reflected fields]. The reflected pulse has developed a double-peaked structure (solid line), and become significantly chirped (dashed line). In particular, the central portion of the pulse has a peak local wavelength of 990 nm , a significant redshift. This redshift is also evident in the reflected pulse spectrum (solid line) shown in Fig. 1(c) corresponding to Fig. 1(b), along with considerable spectral broadening and modulation (the input spectrum is shown by the dashed line and is associated with the left-hand scale).

The results shown in Fig. 1 are typical of what we observe in our simulations in the nonlinear regime, namely, distortion of the reflected field profile and significant spectral modulation and associated redshift. To expose the physics underlying these phenomena we show in Figs. 2(a) and 2(b) the spatial distribution of the full field and the population difference $n = \rho_{22} - \rho_{11}$ at various times corresponding to the results shown in Fig. 1. Figure 2(a) shows that the field penetrates progressively further into the interface as the absorption is saturated,

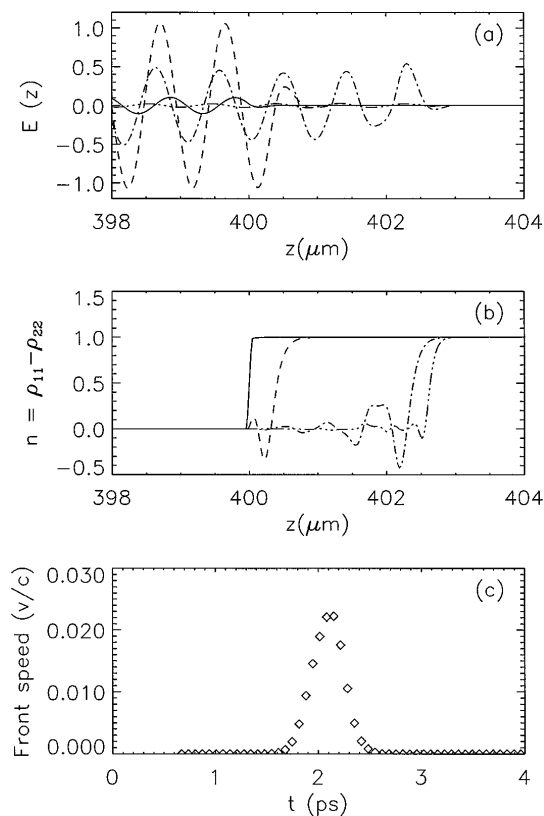


FIG. 2. Spatial distribution of (a) the full field in the vicinity of the interface at $z_0 = 400 \mu\text{m}$, and (b) the population difference n at times $t = 1.61$ ps (solid line), 1.95 ps (dashed line), 2.28 ps (single-dotted-dashed line), and 2.62 ps (triple-dotted-dashed line), where the front propagates to the right with increasing time, and (c) the numerically calculated absorption front velocity normalized to c .

as can be seen by comparing the field profiles at $t = 1.61$ ps (solid line) and $t = 1.95$ ps (dashed line) or $t = 2.28$ ps (single-dash-dotted line) (at $t = 2.62$ ps, the field has been mostly reflected). At $t = 1.61$ ps (solid line), Fig. 2(b) shows that $n = 0$ before the interface signifying zero absorption, and $n = 1$ beyond the interface signifying large absorption due to the two-level systems. At later times, after the input pulse has penetrated into the interface, the population difference is depleted, and the absorption front is seen to propagate into the nonlinear medium. The propagating absorption front maintains a sharp wavelength scale transition region so that the linear skin effect still occurs but now from a moving absorption front. Thus the self-reflected field must suffer a redshift due to the Doppler effect, akin to the reflection from a mirror moving away from a source [5]. To validate this physical picture we have determined the absorption front velocity from the numerical simulation in Fig. 2(b), and the result is shown in Fig. 2(c). After initially accelerating, the front reaches a maximum velocity of $v_{\text{max}}/c = 0.023$ before decelerating back to zero velocity. The maximum wavelength shift of the reflected

pulse due to the Doppler effect is then $\Delta\lambda/\lambda_0 = 2v_{\text{max}}/c$ for $v_{\text{max}}/c \ll 1$ [5], or $\Delta\lambda = 43$ nm for the free-space wavelength $\lambda_0 = 942$ nm used here. Thus, based on the Doppler effect, we expect a maximum local wavelength of $\lambda = 985$ nm, in good agreement with the numerical results in Fig. 1(b). The Doppler effect, upon reflection from the moving absorption front, can therefore explain the magnitude of the observed pulse wavelength chirp.

We are now in a position to further explain the physics underlying the pulse profiles and spectra in Fig. 1: As the leading edge of the input field penetrates into the medium the absorption front accelerates and the local wavelength of the reflected field increases, and on the trailing edge of the pulse the absorption front decelerates and the local wavelength decreases. This explains the initial rise and then decrease in the wavelength chirp in Fig. 1(b) (dashed line). Note that the field profile in Fig. 1(b) (solid line) exhibits a minimum at the same point that the local wavelength peaks, and this begs a physical explanation. A graph of the cw intensity reflectivity of the linear interface [12], for the same parameter values used to generate Figs. 1 and 2, shows that the reflectivity decreases, relative to the pulse center wavelength $\lambda_0 = 942$ nm, for wavelengths red detuned from the resonance. This is so because, even though the absorption decreases, the skin depth increases, thus allowing more path length in the medium over which absorption of the field can occur (the situation is more complicated for blue detuning, but that does not concern us here). Thus the redshifted peak portion of the reflected pulse in Fig. 1(b) experiences a lower reflectivity than the wings, giving rise to the double-peaked reflected field. More quantitatively, for the maximum redshifted wavelength of $\lambda = 985$ nm the reflectivity is reduced to 2%. This can also be intuited by realizing that a redshift of $\Delta\lambda = 43$ nm corresponds to 4.6 linewidths (γ_2), and a significant reduction in absorption and reflection is to be expected. Furthermore, this physical picture correctly indicates that for lower input fields the Doppler shift is reduced, in which case the differential reflection coefficient between the wings and center of the pulse need not be as large as in Fig. 1(b). In this case, the reflected pulse can be single peaked, though still redshifted.

An experimentally measurable signature of the double-peaked reflected field in Fig. 1(b) is the modulated spectrum in Fig. 1(c). The reflected field is composed of two peaks with a spacing $\Delta z \approx 100 \mu\text{m}$. Treating these as point sources in z , we expect a modulation in the wavelength spectrum with a period $d \approx \lambda_0^2/\Delta z = 0.009 \mu\text{m}$, which agrees reasonably with the modulation period in Fig. 1(c). In the case that the reflected field is single peaked, the reflected spectrum is redshifted, but with no modulation.

While the slowly-varying envelope approximation (SVEA) [4,12], cannot capture the physics of the evolution of the self-reflected wave, we can employ it to demonstrate front propagation in the medium

away from the interface. In particular, we introduce the field and polarization envelopes via the definitions $E = 1/2[A_E \mathcal{E} \exp\{i(kz - wt)\} + \text{c.c.}]$ and $P = 1/2[A_P \mathcal{P} \exp\{i(kz - wt)\} + \text{c.c.}]$, where $A_E = \hbar(\gamma_1 \gamma_2)^{1/2}/p$ and $A_P = -iNp(\gamma_1/\gamma_2)^{1/2}$, to obtain the usual Maxwell-Bloch equations in the SVEA from Eqs. (1) and (2) [10]. For the case considered here with $T_1 \gg t_0 > T_2$, we may ignore the population relaxation, and in the limit of small T_2 , we may adiabatically eliminate the polarization. We then obtain the pair of coupled equations

$$\frac{\partial I}{\partial z} + \frac{1}{c} \frac{\partial I}{\partial t} = -\frac{\alpha}{2} nI, \quad \frac{\partial n}{\partial t} = -\gamma_1 nI, \quad (5)$$

where $I = |\mathcal{E}|^2$. These equations admit traveling wave solutions depending solely on the variable $\eta = t - z/v$, where v is the front velocity [8]. Assuming a pulse profile with $I(-\infty) = 0$ and $I(\infty) = F^2$, a constant, and a corresponding bleaching of the two-level system inversion from the ground state to transparency, $n(-\infty) = 1$ and $n(\infty) = 0$, we find the front solution

$$I(\eta) = \frac{F^2}{2} [\tanh(\eta/\eta_0) + 1],$$

$$n(\eta) = \frac{1}{2} [1 - \tanh(\eta/\eta_0)], \quad (6)$$

where $c\eta_0 = 2c/\gamma_1 F^2$ is the characteristic spatial width of the traveling wave front, and the front velocity is given by $c/v = 1 + \omega\psi/\gamma_1 F^2$ [8,9]. For the parameters above, this gives $v/c = 0.026$, which is smaller than the value reported above due to neglect of the self-reflected wave in the present calculation. Thus we have analytic confirmation that absorption fronts can propagate in the nonlinear medium, and we identify these with the fronts seen in our numerical simulations. We further note that numerical integration of the full SVEA equations also clearly shows front propagation for these parameters, but with a damped, oscillatory front profile.

The nonlinear skin effect appears over a much broader range of parameters than employed here. As in the cw case we require the dimensionless parameters ψ and F to be larger than unity so that there is a linear skin effect and a high enough level of nonlinear absorption saturation. In particular, we note that, especially for longer pulses, F can be substantially smaller than the value of $F = 320$ in the example above, though the front velocities and spectra are correspondingly reduced. For the pulse duration and material relaxation times, we require $T_1 \gg t_0 > T_2$ to obtain propagating absorption fronts, where the condition $t_0 > T_2$ is imposed to avoid the regime of self-induced transparency (the input pulse area above is $\mathcal{A} = 1.76pE_0 t_0/\hbar = 10.8\pi$) [13]. Given these restrictions,

excitonic resonances in quantum well materials are prime candidates for the observation of this effect, where high absorptions and suitable relaxation times are available [3]. The remaining questions are then whether the high levels of saturation can be achieved, and if, under these conditions, simple two-level polarization dynamics can be realized.

In conclusion, we have introduced the dynamic nonlinear optical skin effect for reflection of pulses from a highly absorbing interface. This new basic effect for the electrodynamics of interfaces combines the concepts of self-reflected waves [4] and front propagation, and is also a prime example of a nonlinear optical phenomenon where the SVEA fails and the full Maxwell equations must be employed. We have shown that the nonlinear optical skin effect arises from moving absorption fronts so that the red-shifting and spectral modulation of the reflected pulse are clear experimental signatures of the effect.

We thank Dr. Robert Indik for constructive discussions and suggestions. E. M. W. would like to thank Professor Ray Chiao, Professor Alex Kaplan, Professor John McCullen, Professor Pierre Meystre, and Dr. John Garrison for their insightful remarks concerning this work. The authors also wish to thank the Arizona Center for Mathematical Sciences (ACMS) for support. ACMS is sponsored by AFOSR Contracts No. F49620-94-1-0463 and No. F49620-94-1-0051. E. M. W. is partially supported by the Joint Services Optical Program.

*Electronic address: wladek@acms.arizona.edu

- [1] L. D. Landau, E. M. Lifshitz, and L. P. Pitaevskii, *Electrodynamics of Continuous Media* (Pergamon Press, Oxford, 1984), 2nd ed., pp. 208–210.
- [2] M. Born and E. Wolf, *Principles of Optics* (Pergamon Press, Oxford, 1989), 6th ed., pp. 611–664.
- [3] N. Peyghambarian, S. W. Koch, and A. Mysyrowicz, *Introduction to Semiconductor Optics* (Prentice-Hall, Englewood Cliffs, NJ, 1993).
- [4] L. Roso-Franco, Phys. Rev. Lett. **55**, 2149 (1985).
- [5] A. Sommerfeld, *Optics* (Academic Press, San Diego, 1949), pp. 72–75.
- [6] L. Roso-Franco and M. L. Pons, Opt. Lett. **15**, 1230 (1990).
- [7] S. R. Hartmann and J. T. Massanah, Opt. Lett. **16**, 1349 (1991).
- [8] E. Hudis and A. E. Kaplan, Opt. Lett. **19**, 616 (1994).
- [9] A. E. Kaplan and P. L. Shkolnikov, Phys. Rev. Lett. **75**, 2316 (1995).
- [10] A. C. Newell and J. V. Moloney, *Nonlinear Optics* (Addison-Wesley, Redwood City, 1992), Chap. 4.
- [11] K. S. Yee, IEEE Trans. Antennas Propag. **14**, 302 (1966).
- [12] L. Roso-Franco, J. Opt. Soc. Am. B **4**, 1878 (1987).
- [13] L. Allen and J. H. Eberly, *Optical Resonance and Two-Level Atoms* (Wiley, New York, 1975).